ISSN 0915-633X

INTERNATIONAL ATOMIC ENERGY AGENCY

THIRTEENTH INTERNATIONAL CONFERENCE ON
PLASMA PHYSICS AND CONTROLLED NUCLEAR FUSION RESEARCH

Washington, DC, United States of America, 1–6 October 1990

IAEA-CN-53/C-1-4

NATIONAL INSTITUTE FOR FUSION SCIENCE

Confinement Characteristics of High Power Heated Plasma in CHS

O. Kaneko, S. Kubo, K. Nishimura, T. Shoji, M. Hosokawa, K. Ida, H. Idei, H. Iguchi, K. Matsuoka, S. Morita, N. Noda, S. Okamura, T. Ozaki, A. Sagara, H. Sanuki, C. Takahashi, Y. Takeiri, Y. Takita, K. Tsuzuki, H. Yamada, T. Amano, A. Ando, M. Fujiwara, K. Hanatani, A. Karita, T. Kohmoto, A. Komori, K. Masai, T. Morisaki, O. Motojima, N. Nakajima, Y. Oka, M. Okamoto, S. Sobhanian and J. Todoroki

(Received – Aug. 28, 1990)

NIFS-39 Sep. 1990

RESEARCH REPORT
NIFS Series

NAGOYA, JAPAN

INTERNATIONAL ATOMIC ENERGY AGENCY

THIRTEENTH INTERNATIONAL CONFERENCE ON
PLASMA PHYSICS AND CONTROLLED NUCLEAR FUSION RESEARCH

Washington, DC, United States of America, 1–6 October 1990

IAEA-CN-53/C-1-4

CONFINEMENT CHARACTERISTICS OF HIGH POWER HEATED PLASMA IN CHS

O.Kaneko, S.Kubo, K.Nishimura, T.Shoji[*)], M.Hosokawa, K.Ida, H.Idei, H.Iguchi, K.Matsuoka, S.Morita, N.Noda, S.Okamura, T.Ozaki, A.Sagara, H.Sanuki, C.Takahashi, Y.Takeiri, Y.Takita, K.Tsuzuki, H.Yamada, T.Amano, A.Ando, M.Fujiwara, K.Hanatani[$)], A.Karita, T.Kohmoto, A.Komori[+)], K.Masai[*)], T.Morisaki[+)], O.Motojima, N.Nakajima, Y.Oka, M.Okamoto, S.Sobhanian[#)], J.Todoroki

National Institute for Fusion Science, Nagoya 464-01, Japan

[*)] *Plasma Science Center, Nagoya University, Nagoya, Japan*

[$)] *Plasma Physics Laboratory, Kyoto University, Uji, Japan*

[+)] *Interdisciplinary Graduate School of Engineering Science, Kyushu University, Fukuoka, Japan*

[#)] *Department of Physics, University of Tabriz, Tabriz,Iran*

13th International Conference on Plasma Physics
and Controlled Nuclear Fusion Research
Washington DC, USA, 1-6 Oct. 1990
IAEA-CN-53/C-1-4

CONFINEMENT CHARACTERISTICS OF HIGH POWER HEATED PLASMA IN CHS

ABSTRACT

High-power-heated discharges in CHS are studied from the view point of optimizing the plasma performance in low-aspect-ratio heliotron/torsatron (R/a=100cm/20cm). With tangential neutral injection, the stored energy, especially the electron temperature, strongly depends on the location of magnetic axis. The optimal magnetic axis (R_{ax}=92cm), however, does not coincide with the location where the theory predicts the most favorable drift surface (R_{ax}=88cm). High beta plasma ($<\beta>$=1.5%) can also be obtained in inward shifted configurations at the toroidal field B_t=0.47-0.6T. The optimal location is also R_{ax}=92cm although the observed plasma center shifts outward by several cm due to Shafranov shift. So far, the obtained stored energy stays in the range that the LHD scaling predicts. This fact means that the performance of CHS, i.e. low-aspect-ratio helical system, is as good as other helical systems. The induced currents are observed both in ECH and NBH discharges. In NBH discharges, the currents consist of bootstrap and OHKAWA currents. In fact, the current reversal is often observed when the density is high or B_t is low, which is consistent with the theory of bootstrap current in the plateau regime.

KEYWORDS: helical system, confinement, high beta, OHKAWA current, bootsrap current

1. Introduction

Helical systems are attractive because of their potential of steady state, current-disruption-free operation. Recent technical development on plasma production and heating has made it possible to realize a high performance plasma. Then the issues on designing optimal helical system comes from its wide variety of configurations. The low-aspect-ratio heliotron/torsatron configuration is recently paid attention because of its compact size and the potential of high MHD stability [1]. Although the size of loss cone and the fragility of magnetic surface are concerned as possible problems in this configuration, recent theoretical studies suggest that the additional dipole and/or quadrupole magnetic field components improve the situation [2].

The CHS (Compact Helical System) is the medium-sized heliotron/torsatron device (R=1m/a=0.2m) with ℓ=2 and m=8. It is characterized by its low aspect ratio of 5 [3-5]. The major objectives of CHS experiments are therefore placed on a study of transport phenomena and MHD characteristics to optimize low-aspect-ratio helical system.

2. Experimental Setup

Plasma production and heating are performed by ECH with fundamental (28GHz, 120kW) and/or second harmonic (53.2GHz, 150kW) resonances. Plasma production by ICRF (7.5-18MHz, 350kW) is also available. The additional heating is carried out by NB (40keV, 1.1MW, 1sec.) with scannable injection angle. ICRF plasma production is a useful tool because it has a wide operating region on the toroidal field B_t as shown in Fig.1. With Titanium

(Ti) gettering a high power tangential neutral injection can sustain the discharges started by ICRF. Therefore the operating toroidal field strength of CHS is not limited by ECR condition.

CHS has a poloidal coil system that can change a dipole and a quadrupole magnetic field components independently. The shape and the location of plasma can be varied by these coils. With a scannable neutral beam injector, it is possible to optimize the power deposition profile for each configuration.

Main diagnostics of CHS are: HCN laser interferometry for density measurement, a diamagnetic loop for stored energy, Thomson scattering for spatial profiles of electron temperature and density, charge-exchange recombination spectroscopy (CXRS) for spatial profiles of ion temperature and rotation, and VUV spectroscopy for impurity behavior. A visible spectroscopy, a Rogowsky coil and magnetic probes are also used.

3. High Power Neutral Beam Heated (NBH) Discharge

CHS has a single neutral beam line which can deliver 40keV, 1.1MW hydrogen beam through the port for one second. The injection angle can be varied from normal to tangential direction by rotating the whole beam line [6]. The experiments started by tangential injection because of the lack of armor plate and the expected good beam deposition and confinement.

The plasma was able to be sustained by NI alone from the first trial. Both ECRH and ICRH are available for production of target plasma for NI. However, the operation is sensitive to the wall condition. Ti gettering is essential to increase the operational range of density or pulse length [7]. By Ti

gettering, which covers more than 85% of the wall, the line average density $\bar{n}_e$ of 8 x 10^{19} m^{-3} was achieved. The radiation power is 10-20% of absorbed power for $\bar{n}_e$<5 x 10^{19} m^{-3}, while it increases up to 50% for $\bar{n}_e$=8 x 10^{19} m^{-3}, where the radiation loss is mainly due to oxygen in high density plasma. Oxygen is also a dominant impurity at the radiation collapse which limits the maximum density. The obtained density is still below the scaling [8]. The plasma can be sustained up to 800ms under the moderate density of 3 x 10^{19} m^{-3} almost steadily.

The plasma stored energy W_p by the diamagnetic coil roughly agrees with the LHD scaling [8]. Figure 2 shows the comparison of experimental data with the LHD scaling: $W_p(kJ)=\alpha*P_{abs}(MW)^{0.42}*\bar{n}_e(10^{20}m^{-3})^{0.69}*B_t(T)^{0.84}*a(m)^{2.0}*R(m)^{0.75}$, where P_{abs} is the absorbed power and the coefficient α is 170. The experimental data show a weaker density dependence as $\bar{n}_e^{0.6}$.

4. Magnetic Axis Shift Experiments

The magnetic field configuration varies as the location of the magnetic axis by controlling a magnetic dipole field. In CHS the magnetic axis (in vacuum) R_{ax} can be varied from 88.8 to 101.6 cm. Generally speaking, the outward shift increases magnetic well and makes divertor configuration, while the inward shift increases magnetic shear and improves high energy particle confinement. Indeed, NBH plasmas are affected strongly by the shift of magnetic axis.

Figure 3 shows the dependence of W_p on R_{ax} for NBH plasma under the same injection power. The maximum stored energy can be obtained at R_{ax}=95cm. Because the plasma volume also changes as

the magnetic axis shifts, the stored energy is normalized by the volume to eliminate the volume effect on confinement. This is also shown in Fig.3. Then the optimal position is R_{ax}=92cm. The finite-β plasma axis R_0 differs from R_{ax} due to Shafranov shift which is large in the low-aspect-ratio machine. In the case of Fig.3, the optimum position corresponds to $R_0 \approx 95$cm where the field ripple is almost zero on the axis. Figure 4 shows the behavior of the central electron temperature $T_e(0)$ as a function of electron density. At the same density, $T_e(0)$ is largest when R_{ax}=92cm. So far we cannot measure $T_e(0)$ for $R_{ax}<92$cm. As for the beam deposition, the orbit loss of fast ions varies only from 10% to 20% as the axis goes 92.1cm through 101.6cm. Therefore these results show that the confinement, at least in the core, is improved as the magnetic axis shifts inward down to 92cm. This improvement can also be seen in Fig.2, where the data show that the coefficient of LHD scaling α depends on R_{ax}.

This tendency is not yet clearly understood. From the view point of particle orbit, the deviation of drift surface from magnetic surface becomes minimized at R_{ax}=89cm. On the other hand, the interference between plasma and the inner wall becomes stronger when the plasma moves inward ($R_{ax}<98$cm). In fact the attainable density is limited by radiation collapse for $R_{ax}<92$cm. Therefore the strong plasma wall interaction might spoil the good confinement of fast ions. This kind of dependence is not clearly seen for ECH plasma ($88.8\text{cm} < R_{ax} < 97.4\text{cm}$), where it is difficult to estimate the change of power deposition profile.

The local transport analysis has been done based on the measured density and temperature profiles using ORNL PROCTR-mod

code [9]. The typical values of obtained electron thermal conductivity χ_e are 2-10 m^2/s for both NBH and ECH plasmas in spite of different plasma parameters and collisionality [5]. The anomaly compared with neoclassical value appears to be higher when the electron density is high. In CHS the ion temperature profile can be obtained by CXRS for NBH plasmas. However, the estimate of ion thermal conductivity χ_i is more ambiguous because of the lack of Z_{eff} measurement. Assuming that $Z_{eff}=2$ and is uniform, χ_i is the same order of χ_e and is also anomalous.

5. High Beta Study

One of the motivations of studying low-aspect-ratio helical system is in its good MHD stability for high β plasma. The theoretical prediction based on H-APOLLO and H-ERATO codes shows that the β limit also depends on the location of magnetic axis. The β is limited by stability for $R_{ax}<92$cm because of magnetic hill configuration, and by equilibrium for $R_{ax}>92$cm because of large shift of magnetic axis and small plasma cross section. The predicted maximum β of 6% is thus attained at $R_{ax}=92$cm for a parabolic pressure profile.

The experiments have been done at $B_t=0.45$-0.6T by ECH (28GHz, second harmonic) or ICRF (7.5MHz) start-up. From the diamagnetic measurement, the volume averaged beta of 1.5% is achieved including the beam pressure. The attained beta are almost the same for $B_t=0.45$-0.6T because the plasma performance degrades as B_t. The obtained density and temperature profiles show a large Shafranov shift. The finite beta equilibrium is consistently obtained by PROCTR-mod and VMEC using these

profiles. Figure 5 shows the calculated equilibrium beta values using observed pressure profile at different magnetic axis. A similar R_{ax} dependence of β as Fig.3 can be seen in this low toroidal field operation. MHD activities of low m/n coherent modes are observed during operation. The amplitude becomes large as the magnetic axis shifts inward, but it still remains on a low level.

6. Induced Currents

Because CHS has a single beam line, and the beam is injected tangentially in most experiments, a large amount of beam driven current is expected. However in CHS, the behavior of measured current is more complicated. Figure 6 shows typical time evolutions of plasma current in three cases. When the density is low, a large current of up to 15kA is observed in the same direction as beam injection (a). When the density is high (b) or B_t is low (c), the current flows reversely, i.e. in the counter direction. (Note that the current does not reach the steady state especially in the low density discharge because the slowing down time is long and the magnetic diffusion time is also long due to high temperature.) The reversed current also appears when the injection angle is varied from tangential to normal direction. This result suggests that the observed currents consist of two components, one of which is a beam driven OHKAWA current and the other is the bootstrap current.

When the density is low, the parameter dependence of currents fits the one of beam driven; $I_p \propto P_{abs} * \langle T_e \rangle / \bar{n}_e / R$. Subtracting the beam driven component using this formula, the

amount of bootstrap component is 2-4 kA. This value and the direction as well agree with the theoretical prediction of the bootstrap current in the plateau regime [10]. No reversed currents are observed in the counter-injection experiments because both the beam driven and the bootstrap currents flow in the same direction in this case.

The induced currents are also observed in ECH plasma. The direction of currents is co-direction, and its amount depends on the magnetic quadrupole field. When the cross section of plasma is elongated vertically, the amount of current decreases and the direction is reversed in some cases. These results are consistent with the theory of the bootstrap current in the collisionless regime.

So far the induced current does not affect the global confinement characteristics.

7. Summary and Conclusion

The survey of the characteristics of tangential NBH plasma has been performed in CHS. Although it was worried that the confinement of fast ions was not good in the low-aspect-ratio machine, the experimental results show that the obtained performance of plasma is as good as those of other helical systems. The location of magnetic axis is a very important parameter to optimize the global confinement characteristic. The higher pressure plasma can be obtained as the magnetic axis shifts inward down to R_{ax}=92cm. The more shift degrades the operating density limit, which suggests that the plasma wall interaction (at the inner wall) may occur. The similar tendency

can also be found in the low toroidal field operation. Indeed, the highest beta value of 1.5% is also obtained in the inward shifted configuration. Although the MHD activities are observed in the high β operation, they don't seem to affect the confinement. So far the beta value is limited by heating power.

The observed currents can be explained by the beam driven and the bootstrap currents in the plateau regime for NBH plasma. The efficiency of the beam driven current seems to be the same order as in tokamaks. The theoretically predicted bootstrap current can explain the experimental results. The behavior of the currents observed in ECH collisionless plasma also agrees with the bootstrap theory.

REFERENCES

[1] SHEFFIELD, J., et.al., Fusion Technol. 9 p199 (1986)

[2] CARRERAS, B. A., et.al. Nucl. Fusion 28 p1195 (1988)

[3] MATSUOKA, K., et al., Plasma Physics and Controlled Nuclear Fusion Research (Proc. 12th IAEA Conf., Nice) p411 (1989)

[4] OKAMURA, S., et al., Controlled Fusion and Plasma Physics (Proc. 16th Eur. Conf., Venice) p571 (1989)

[5] IGUCHI, H., et al., Controlled Fusion and Plasma Physics (Proc. 17th Eur. Conf., Amsterdam) p451 (1990)

[6] KANEKO, O., et.al., in Proc. 13th Symp. on Fusion Engineering, Knoxville p1455 (1989)

[7] NODA, N., et al., in Proc. of 9th PSI Conf., Bournemonth (1990), to be published in J. of Nucl. Mater.

[8] SUDO, S., et al., Nucl. Fusion 30 p11 (1990)

[9] HOWE, H.C., ORNL/TM-9537, Martin Marietta Energy Systems, Oak Ridge Natl. Lab., (1985)

[10] SHAING, K.C., HIRSHMAN, S.P., and CALLEN, J.D., Phys. Fluids, 29 p521 (1986)

Figure Captions

Fig.1 The line averaged electron density produced with the Nagoya Type-III antenna as a function of the magnetic field strength.

Fig.2 Comparison of the obtained stored energy W_{dia} with the LHD scaling $W_{LHD} \equiv P_{abs} * \tau_{LHD}$ with the location of magnetic axis as a parameter. The range of parameters are:

P_{abs}= 0.2 - 1.0 MW

$\bar{n}_e$ = 0.1 - 0.8 x 10^{20} m^{-3}

R_{ax} = 92 - 101 cm

B_t = 0.98- 1.5 T

Fig.3 Dependence of stored energy (∘) and volume normalized stored energy (•) on the location of magnetic axis. B_t=1.05T, P_{in}=1MW, Co-injection.

Fig.4 Dependence of the central electron temperature on the electron density at four different locations of magnetic axis. Circles and squares correspond to the different injection angles of NBI, where the R_{tan} indicates the tangency radius of the beam.

Fig.5 The equilibrium beta values that are obtained at different magnetic axis. Arrows show the Shafranov shift. Theoretical equilibrium and stability limits are also shown, which are calculated under the fixed boundary conditions by H-APOLLO and H-ERATO codes, respectively.

Fig.6 Typical time evolutions of plasma current and line average density in three different cases: low density, high density and low B_t.

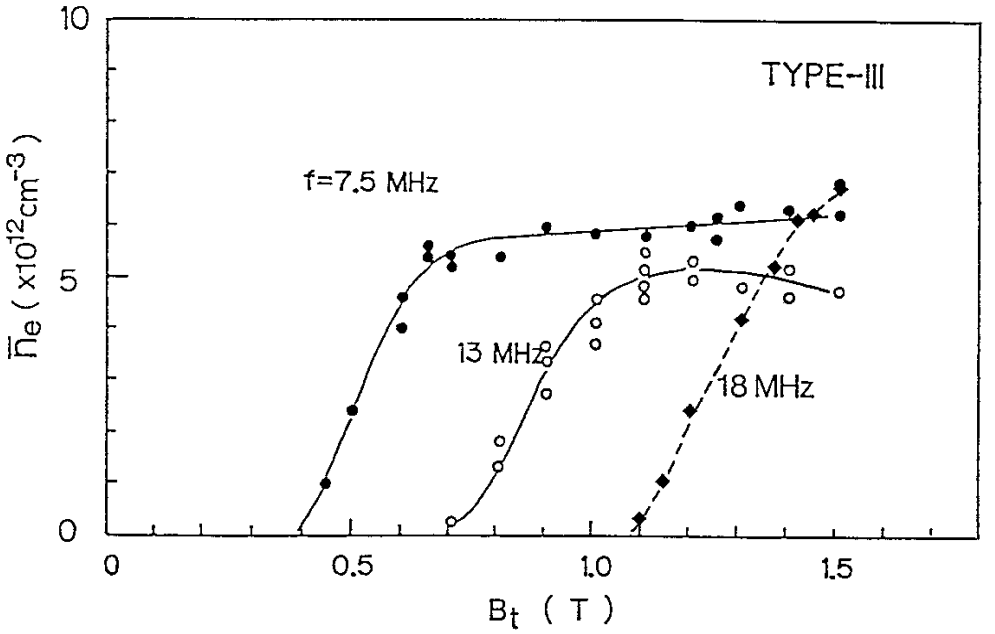

Fig.1 The line averaged electron density produced with the Nagoya Type-III antenna as a function of the magnetic field strength.

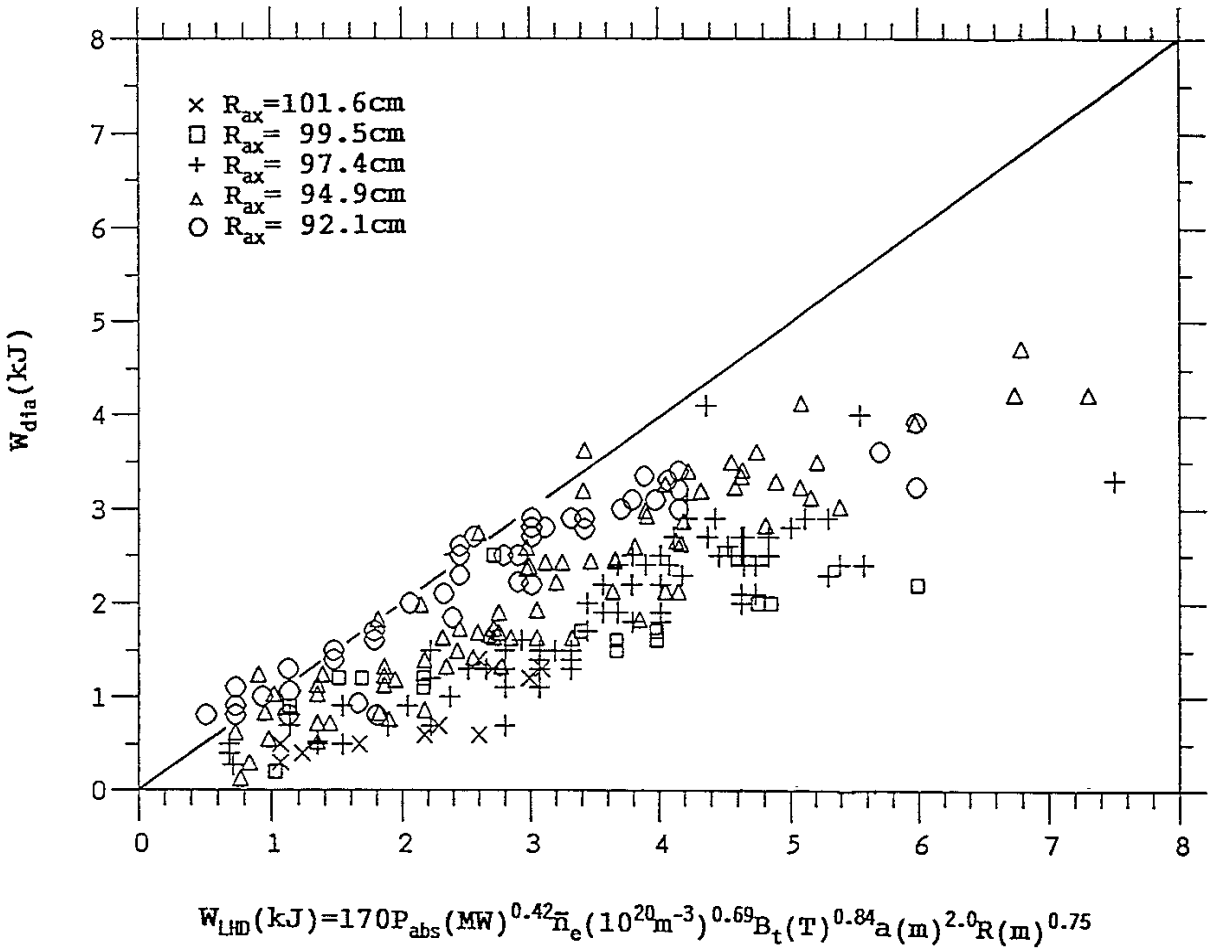

Fig.2 Comparison of the obtained stored energy W_{dia} with the LHD scaling $W_{LHD} \equiv P_{abs} * \tau_{LHD}$ with the location of magnetic axis as a parameter. The range of parameters are:

P_{abs}= 0.2 - 1.0 MW

$\bar{n}_e$ = 0.1 - 0.8 x 10^{20} m^{-3}

R_{ax} = 92 - 101 cm

B_t = 0.98- 1.5 T

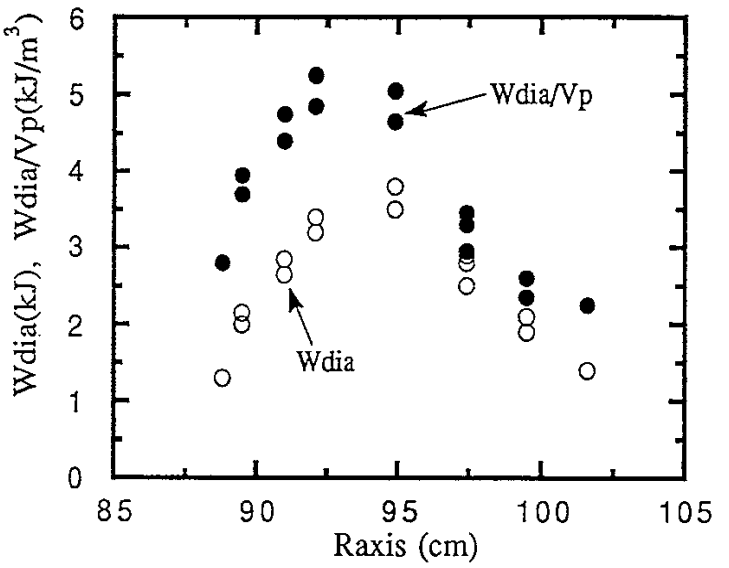

Fig.3 Dependence of stored energy (∘) and volume normalized stored energy (•) on the location of magnetic axis.

B_t=1.05T, P_{in}=1MW, Co-injection.

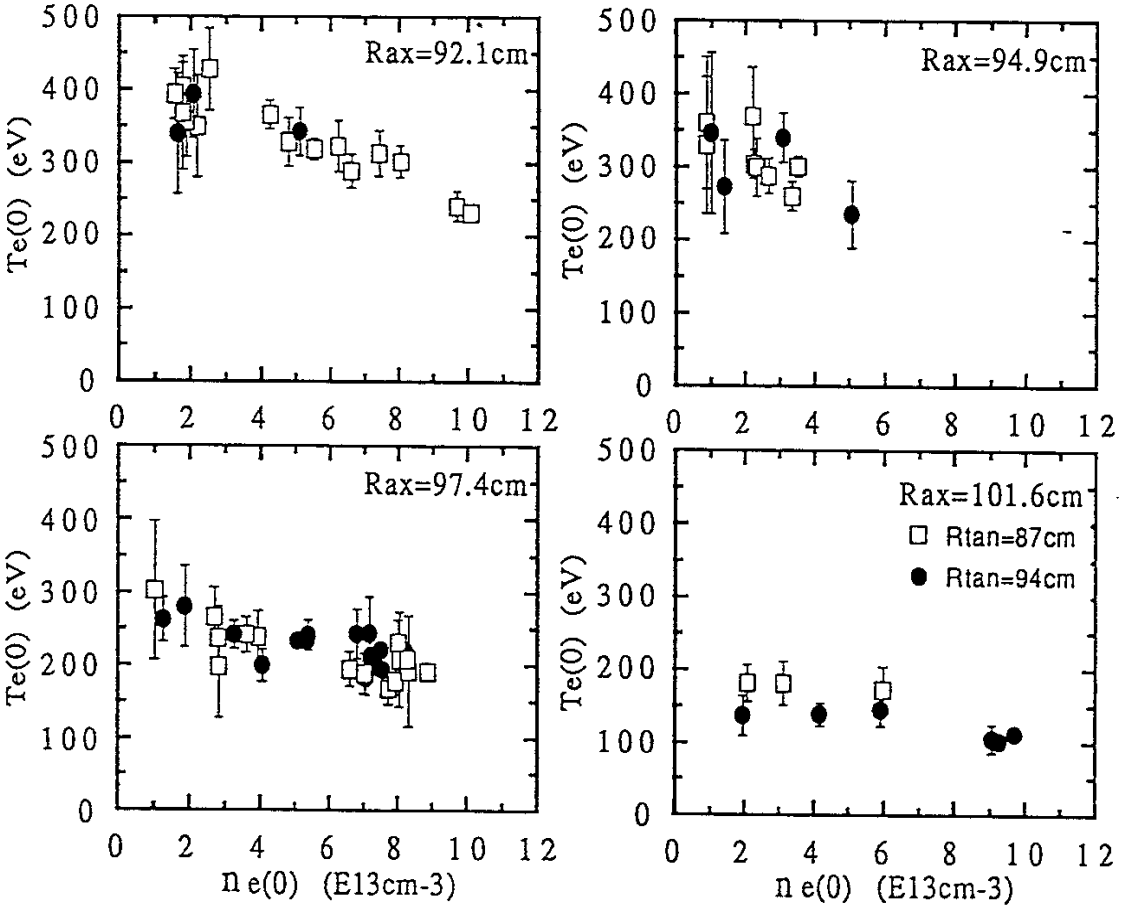

Fig.4 Dependence of the central electron temperature on the electron density at four different locations of magnetic axis. Circles and squares correspond to the different injection angles of NBI, where R_{tan} indicates the tangency radius of the beam.

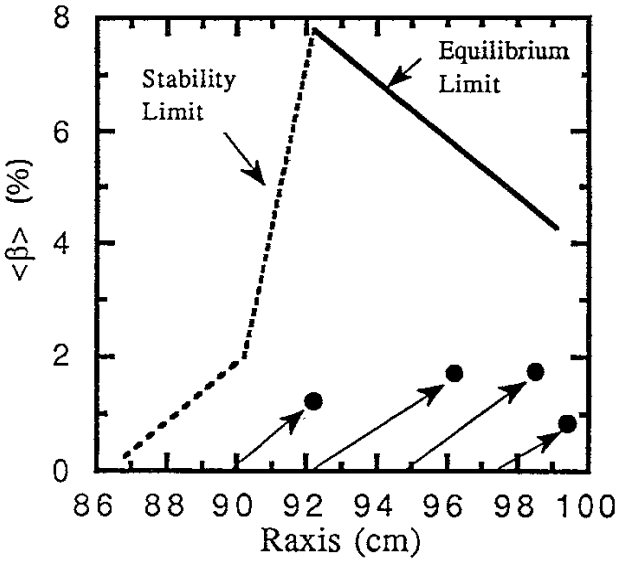

Fig.5 The equilibrium beta values that are obtained at different magnetic axis. Arrows show the Shafranov shift. Theoretical equilibrium and stability limits are also shown, which are calculated under the fixed boundary conditions by H-APOLLO and H-ERATO codes, respectively.

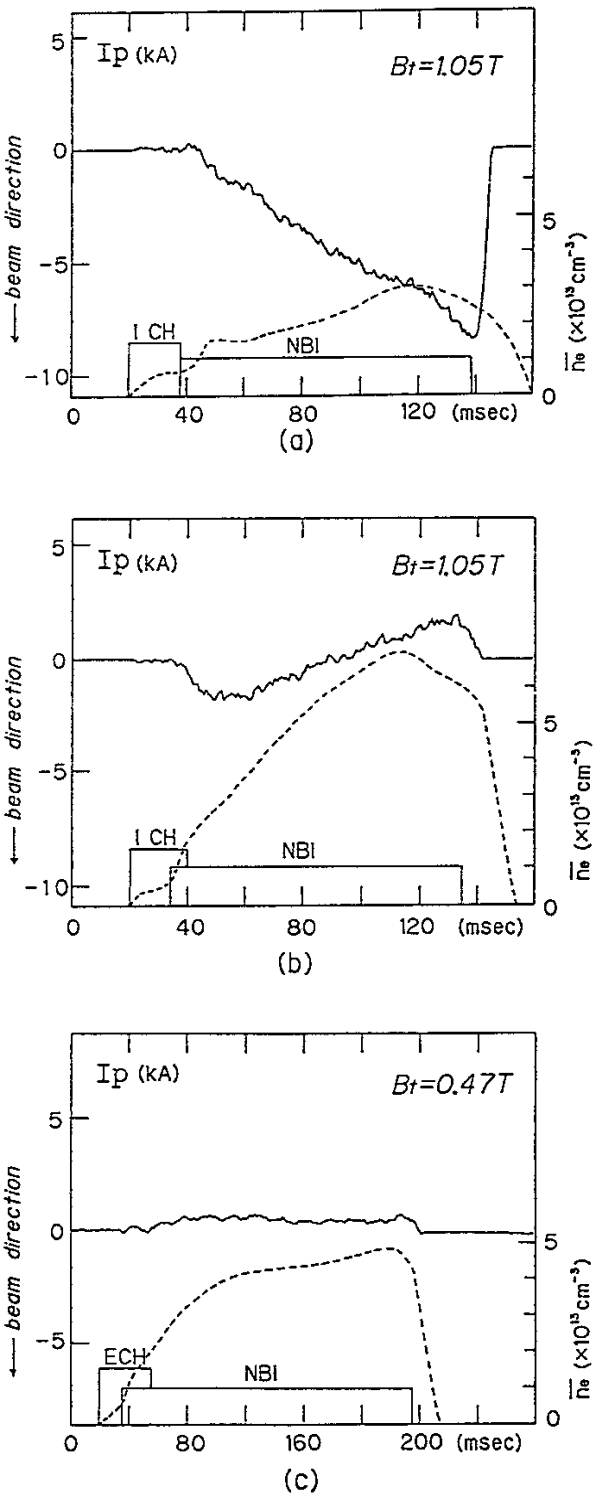

Fig.6 Typical time evolutions of plasma current and line average density in three different cases: low density, high density and low B_t.